



Maximum probing depth of low-energy photoelectrons in an amorphous organic semiconductor film



Yusuke Ozawa^a, Yasuo Nakayama^{a,*}, Shin'ichi Machida^a, Hiroumi Kinjo^a, Hisao Ishii^{a,b}

^a Graduate School of Advanced Integration Science, Chiba University, 1-33 Yayoi-cho, Inage-ku, Chiba 263-8522, Japan

^b Center for Frontier Science, Chiba University, 1-33 Yayoi-cho, Inage-ku, Chiba 263-8522, Japan

ARTICLE INFO

Article history:

Received 16 February 2014

Received in revised form 22 June 2014

Accepted 6 August 2014

Available online 17 August 2014

Keywords:

Attenuation length

Photoemission

Photoelectron yield spectroscopy

Ultraviolet photoelectron spectroscopy

Buried interface

ABSTRACT

The attenuation length (AL) of low energy photoelectrons inside a thin film of a π -conjugated organic semiconductor material, 2,2',2''-(1,3,5-benzinetriyl)-tris(1-phenyl-1-H-benzimidazole), was investigated using ultraviolet photoelectron spectroscopy (UPS) and photoelectron yield spectroscopy (PYS) to discuss their probing depth in amorphous organic thin films. The present UPS results indicated that the AL is 2–3 nm in the electron energy range of 6.3–8.3 eV with respect to the Fermi level, while the PYS measurements which collected the excited electrons in a range of 4.5–6 eV exhibited a longer AL of 3.6 nm. Despite this still short AL in comparison to a typical thickness range of electronic devices that are a few tens of nm-thick, the photoemission signal penetrating through further thicker (18 nm) organic film was successfully detected by PYS. This fact suggests that the electronic structures of “buried interfaces” inside practical organic devices are accessible using this rather simple measurement technique.

© 2014 Elsevier B.V. All rights reserved.

1. Introduction

Interfaces are crucial places where essential processes that dominate the output performance of organic electronic devices occur. Because charge carrier injection into organic semiconducting materials is generally essential for the functioning of organic devices [1], the elucidation of interfacial electronic structures within devices is one of the key issues for understanding and improving device performance. The electronic structures of a wide range of organic materials and their interfaces with conductive substrates have been investigated using photoelectron spectroscopy [2]. The surface sensitivity of this method is, however, problematic if one wishes to probe the *interfaces*. The probing depth of conventional ultraviolet photoelectron spectroscopy (UPS) is approximately 1 nm caused by short attenuation lengths (ALs) of photoelectrons with kinetic energies of 10–50 eV. This surface sensitivity forces researchers to investigate model interfaces consisting of a very thin organic layer deposited on electrodes. Such model systems do not represent the *exact* interfaces found in organic devices due to probable energy shift by screening effects of “photo-holes” [3–5] and/or band bending-like behavior within the organic films [6–8], and thus the investigation of the ‘buried’ interfaces in a deposited thick organic layer, such as those found in real devices, is highly desired.

As a barometer of the probing depth of the electron spectroscopy techniques, the so-called “universal curve (UC)” is commonly adopted, which exhibits an empirically derived relationship between the kinetic energy (E_k) and the inelastic mean free path (IMPF) of electrons in various inorganic and organic solids [9]. Note that the Fermi level is taken as the energy standard of E_k throughout this article. Because it was predicted that the IMPF grows proportionally to E_k^{-2} when E_k is “very low” [9], photons with an energy lower than several eV are expected as promising probes for the investigation of buried interfaces by photoemission [10,11]. In this context, photoelectron yield spectroscopy (PYS), which measures the total photoelectron yield as a function of the incident photon energy (typically 4–9 eV) [11,12], is potentially a suitable technique for surveying the interface electronic structures underneath the few tens of nanometers-thick organic films of actual devices. Other advantages of using PYS are its durability against sample charging [12] and the reduction of “radiation damage” by restricting photoelectron excess energies below 5 eV with respect to the vacuum level [13,14]. These two drawbacks, sample charging and radiation damaging, are inevitable problems with UPS analysis of major organic materials.

The “universality” of the IMFP in the medium- and high-energy regions has been established for both inorganic and organic materials [15–18]. In the low E_k range, however, the cross section of the photoelectron energy loss processes has to be influenced by miscellaneous material-dependent properties e.g. the energy gap width and phonon energy [19], it remains controversial whether

* Corresponding author. Tel.: +81 43 207 3894.

E-mail address: nkym@restaff.chiba-u.jp (Y. Nakayama).

or not the photoelectron AL actually extends along the *universal* trend in the low E_k range [19–21]. In this study, we therefore investigated the AL of low E_k photoelectrons in amorphous films of a typical organic semiconductor material, 2,2',2''-(1,3,5-benzinetriyl)-tris(1-phenyl-1-H-benzimidazole) (TPBi) using both UPS and PYS for the sake of proposing a direct indication of the accessible probing depth within actual organic devices by photoemission-related techniques. As a result, it was demonstrated that PYS can be practically applied for the characterization of buried interfaces.

2. Experimental details

UPS measurements were conducted using two types of energy tunable excitation light sources: synchrotron orbit radiation and a deuterium arc discharge lamp. For the former experiments, photoelectron energy distribution curves were obtained with a concentric hemispherical analyzer (CHA) (ARUPS-10, VG) equipped at the vacuum ultraviolet beam line (BL-8B UVSOR-II), Institute for Molecular Science (IMS), Japan. The excitation energy used in these experiments ranged 20–50 eV. The experimental conditions were identical to those reported previously [2]. The latter UPS experiments were carried out in a home-built system equipped with a retarding field electron analyzer (RFA), where a sample was placed at the center of a hollow hemispherical anode and photoelectrons with a certain E_k were selected by sweeping the retarding electric potential with a small modulation (100 mV, 4.18 Hz) to differentiate the photocurrent using a lock-in amplifier (Stanford Research Systems, model SR830 DSP) after amplification with an ammeter (Keithley, model 6485). The incident photon energy ($h\nu$) was varied from 6.3 eV to 8.3 eV. The photon incident direction was the surface normal, and the measurements were conducted under high vacuum (1.0×10^{-4} Pa) conditions.

PYS measurements were carried out with the same RFA–UPS system [22]. A positive electrostatic potential (+9 V) was applied to the anode to collect all of the emitted photoelectrons. The incident photon energy was swept from 4.0 eV up to 9.3 eV, and the total photocurrent and photon flux were measured using a precise ammeter (Keithley, model 6430) and photomultiplier (Hamamatsu Photonics, R6836), respectively, at each photon energy. The photoelectron yield Y was obtained by dividing the photocurrent by the photon flux.

TPBi was adopted for testing the probing depth inside amorphous organic materials because it is known to generally form pinhole-free flat overlayers when deposited at room temperature [23]. TPBi was evaporated onto Au-coated Si substrates in a step-by-step manner, and photoemission measurements were subsequently conducted throughout in vacuum. The evaporation rate was maintained in the range 0.01–0.03 nm/s, which was monitored with a quartz oscillator and calibrated afterwards using a step profilometer. The pressure during the sample fabrication was 4×10^{-3} Pa for the CHA–UPS experiments and was maintained below 5×10^{-4} Pa for the RFA–UPS and PYS analyses. The film morphology was confirmed to be flat and uniform, as shown in Fig. 1, where no pinhole except several hollows no deeper than 5 nm was found in randomly selected fifteen $100 \mu\text{m}^2$ areas over the film surface, by means of atomic force microscopy (AFM) (SII, SPA-400) in air.

3. Results and discussion

Fig. 2(a) shows the CHA–UPS spectra of a pristine Au substrate and a thick (6.7 nm) overlayer taken at $h\nu = 30$ eV. The threshold edge due to the highest occupied molecular orbital (HOMO) of TPBi was located at a binding energy (BE) of 2.4 eV, which corresponds

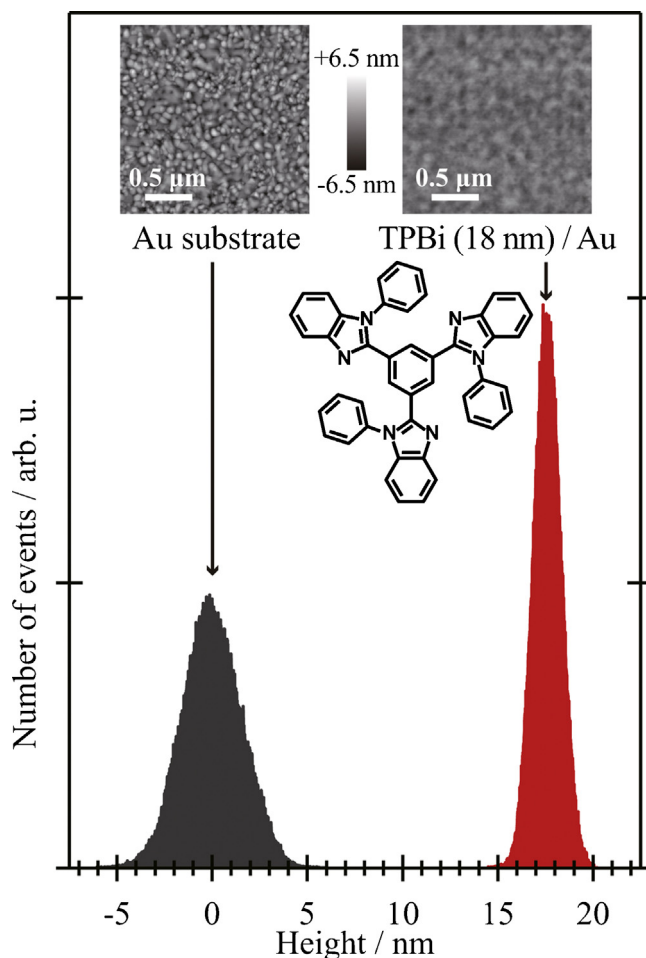


Fig. 1. Typical AFM images of the Au substrate (upper left) and 18 nm-thick TPBi overlayer (upper right) represented together with the height histograms of the respective images. Both AFM images are equally scaled. The molecular structure of TPBi is also shown as the middle inset.

to the hole injection barrier from Au to TPBi. Because the energy gap for TPBi has been reported to be at least 3.5 eV [24], the lowest unoccupied molecular orbital must be located more than 1 eV above the Fermi level. Therefore, the photoelectron signals at the Fermi level ($BE = 0$ eV) were attributed to the Au substrate exclusively.

As shown in Fig. 2(b), the photoelectron intensity of the Fermi edge decayed with increasing overlayer thickness. A photoelectron excited inside a solid loses its energy due to several scattering events with certain probabilities on its way toward the surface. The relative population of the photoelectrons that preserve the primary excitation energy after passing through the solid of a thickness x can be expressed as:

$$\frac{N}{N_0} = \exp\left(-\frac{x}{\lambda}\right), \quad (1)$$

where λ is the AL of the primary electrons which is related to the scattering probability. In the present case, N corresponds to the Fermi edge intensity in the spectrum for the TPBi overlayer with a thickness x , while N_0 is given by the spectrum of the pristine Au substrate ($x = 0$). Fig. 2(c) shows the relative intensity (N/N_0) of the Fermi edge derived from the present CHA–UPS spectra plotted in a semi-logarithmic scale as a function of the TPBi thickness for various excitation energies. These plots show good linearity, suggesting uniform growth of the overlayer. The ALs were determined using the gradients of these plots to be 1.0–1.5 nm for excitation energies of 20–50 eV. In the present UPS works, we only consider

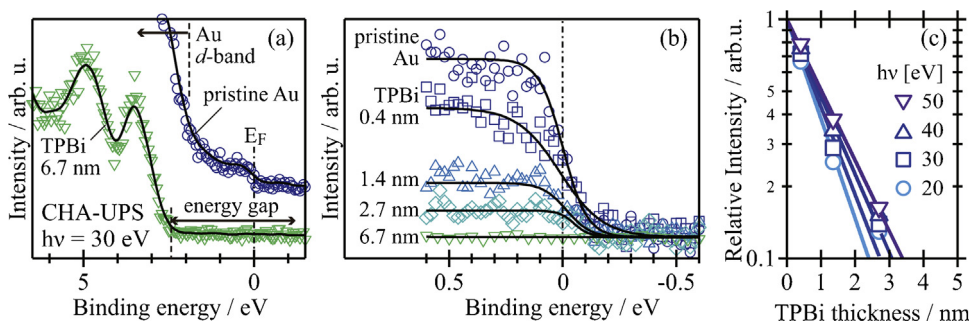


Fig. 2. (a) CHA-UPS spectra of an Au substrate and a 6.7 nm-thick TPBi overlayer taken at $h\nu = 30$ eV. (b) Spectral evolution at the Fermi edge region of TPBi layers of different thicknesses. (c) Relative intensity (N/N_0) of the Fermi edge taken at various excitation energies plotted as a function of the TPBi thickness. The least-squares fitting lines for the respective data sets are also displayed. The line $N/N_0 = 1/e$ was drawn to estimate the ALS.

the photoelectrons excited from the Fermi level (BE = 0 eV) so that the $h\nu$ directly corresponds to the internal kinetic energy of the photoelectrons E_k . Note that N/N_0 decays to less than 1/50 for a 6 nm-thick overlayer even when one assumes the AL to be 1.5 nm. Because such a faint signal is generally under the detection limit of conventional UPS systems as indicated in Fig. 1(b), the maximum accessible probing depth for this technique should be regarded as no greater than 6 nm.

Fig. 3(a) shows the RFA-UPS spectra of the Au substrate and TPBi overlayers taken at $h\nu = 7.8$ eV. From the wide range spectra (not shown), the Au-TPBi hole injection barrier was determined to be $1.77 (\pm 0.15)$ eV. The notable deviation of this value from the result obtained using CHA-UPS may be ascribed to different sample preparation conditions (e.g., the vacuum pressure).

As observed with CHA-UPS, the photoelectron intensity at the Fermi level attenuated with increasing TPBi thickness. In this case, however, a significant contribution of secondary electrons due to inelastic scattering by the overlayer was superimposed on the primary photoelectron signals, resulting in a monotonous slope to the left in the RFA-UPS spectra. This situation makes it difficult to define the Fermi edge intensity by simple curve fitting with the Fermi-Dirac distribution function. Consequently, it was assumed that the Fermi edge intensity could be reasonably derived as the intensity at BE = 0 eV, as indicated on the right axis of Fig. 3(a). In Fig. 3(b)–(d), N/N_0 at BE = 0 eV as a function of the TPBi thickness are displayed for several excitation energies. The AL values were calculated to be 2–3 nm for excitation energies of 6.3–8.3 eV. It should be noted that the ALs did not exhibit a regular dependence on the excitation energy in this case, which is in contrast to the UC that predicts a monotonous increase of the AL with decreasing E_k in this range.

PYS measurements were also conducted on a sample identical to that used for the RFA-UPS analysis. Fig. 4(a) represents the PYS spectra of the pristine Au substrate and deposited TPBi overlayers. Since there is a large energy level offset between the highest occupied electronic states of Au and TPBi as discussed above, the

photoemission signal in the range $h\nu = 4.5$ –6.0 eV can be attributed solely to Au. Although the photoelectron yield in this energy range decayed due to the TPBi overlayer, the photoelectrons from the Au substrate underneath an 18 nm-thick TPBi overlayer were still detectable, as clearly seen in Fig. 3(b). It should also be noted that N/N_0 has to decay down to 1/400 for the 18 nm-thick overlayer if one assumes the AL to be 3 nm based on the aforementioned RFA-UPS analysis.

The photoelectron yield Y just beyond the onset energy is known to be proportional to $(h\nu - E_{th})^n$, where E_{th} is the threshold energy of the photoemission, and $n = 2$ and 3 have been empirically adopted for metals and organic materials, respectively [25,26]. For binary systems of metals and organic materials, the yield can be expressed as a superposition of these two components. In the present case, therefore, photoelectron yield can be simulated as:

$$Y = N_{Au}(h\nu - \varphi_{Au})^2 H(h\nu - \varphi_{Au}) + N_{TPBi}(h\nu - I_{TPBi})^3 H(h\nu - I_{TPBi}), \quad (2)$$

where N_{Au} and N_{TPBi} are proportional constants indicating the signal intensity from Au and TPBi, respectively, φ_{Au} is the work function of Au, I_{TPBi} is the ionization energy of TPBi, and $H(E)$ is the Heaviside step function, whose value switches from 0 to 1 when E turns from negative to positive. For the 18 nm-thick TPBi overlayer (Fig. 3(b)), $\varphi_{Au} = 4.45 (\pm 0.05)$ eV and $I_{TPBi} = 6.25 (\pm 0.12)$ eV are derived from a least-square fitting of the experimental data using Eq. (2), while the residual in the left side of the onset to the TPBi contribution may be ascribed to a tail state derived from the highest occupied state of TPBi. The hole injection barrier of this buried interface underneath the thick TPBi film was determined to be 1.8 eV ($= I_{TPBi} - \varphi_{Au}$), which is in good agreement with the RFA-UPS results for the thinner TPBi overlayers.

The attenuation behavior of the photoelectron yield from Au is shown in Fig. 4(c) together with the other UPS results. The AL was estimated to be 3.6 nm based on the PYS data and is indicated with the plot as a thick line. It should be noticed that, since the

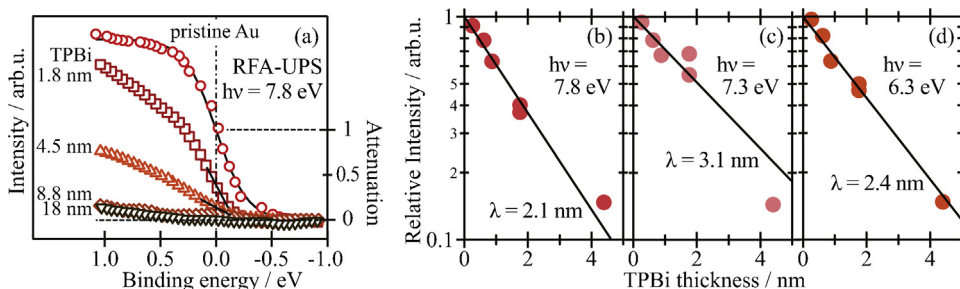


Fig. 3. (a) Evolution of the RFA-UPS spectra at the Fermi-edge region taken at $h\nu = 7.8$ eV. The right axis scale is given to indicate the relative intensity (N/N_0) at the Fermi level. (b)–(d) N/N_0 plotted as a function of TPBi thickness for excitation energies of (b) 6.3, (c) 7.3, and (d) 7.8 eV.

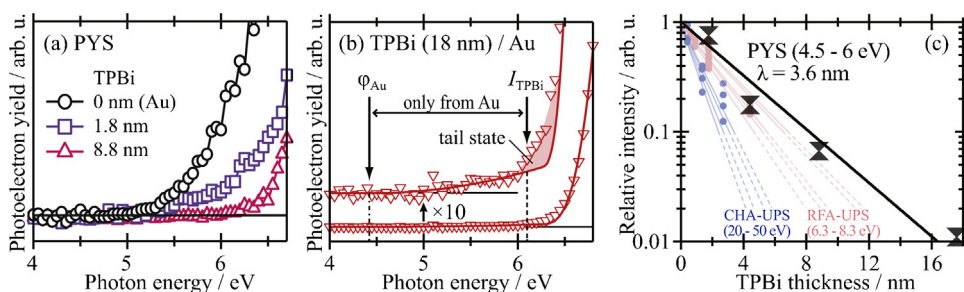


Fig. 4. (a) PYS spectra of an Au substrate and TPBi overlayers. (b) PYS spectra of an 18 nm-thick TPBi overlayer. The vertical scale for the upper plot is extended by ten times to the lower one. The least-squares fitting result for the experimental data using Eq. (2) is represented by the solid curves. The shaded area can be ascribed to tail states above the highest occupied state of TPBi. (c) Relative intensity of N_{Au} derived from the PYS spectra plotted as a function of the TPBi thickness. The least-squares fitting result for this plot using Eq. (1) is indicated by the solid line. Those derived from the present UPS results are also indicated for reference.

present PYS signal from the Au substrate must contain photoelectrons of multiple kinetic energies, this AL value has to be nothing but a *phenomenological* reference of the technique and thus does never correspond to the IMFP of electrons at any specific E_k .

Finally, AL values having been reported by other groups were compared to the present results, which are summarized in Fig. 5. It is clearly seen that, aside from discrepancies to the UC by factor of 2 or less, the present results settle within the range of previous reports. Opposed to the simple E_k^{-2} dependence proposed by Seah and Dench [9], two research groups have reported rather shrinkage of ALs for smaller E_k in the range of 4.5–6 eV for alkane-based molecular layers [19,20]. The conventional UC was also challenged by Graber and co-workers, where they claimed a constant AL value, or at least a much moderate power law ($E_k^{-0.1}$), for $E_k < 200$ eV based on their results for perylene-3,4,9,10-tetracarboxylic dianhydride (PTCDA) thin films [21]. Our present RFA-UPS results which revealed the absence of any clear E_k -AL relationship support this

notion. It is noteworthy that, in spite of considerably weaker E_k dependence for the AL in the low energy region against the orthodox expectation, the present results clearly demonstrate that the maximum probing depth for PYS reaches at least 18 nm. Since the molecular volume of TPBi is estimated to be approximately 1 nm^3 , this probing depth means that buried interfaces far beneath *bulk* organic molecular layers are accessible by this technique. One reason of this long probing depth should be attributed to a principle of the PYS measurement that it does not discriminate primary photoelectrons from scattered ones; in other words, PYS even collects electrons no longer preserving the initial E_k which are abandoned for the UPS measurements. Another important factor is its higher sensitivity in comparison to the conventional UPS, which is also represented in Fig. 4.

4. Conclusion

The accessible probing depth of photoemission-based experimental techniques in the low energy region was revisited using flat overlayers of a typical amorphous organic material TPBi deposited on Au substrates. The UPS results in an excitation energy range of 6.3–8.3 eV revealed a complex E_k -dependence of the photoelectron attenuation length scattering between 2 and 3 nm as opposed to the so-called “universal curve”, while an expected positive E_k -AL was exhibited in the conventional excitation energy range ($h\nu = 20\text{--}50$ eV). Despite the fact that the PYS signals (in the excitation energy range of 4.5–6 eV) also decay by the AL of no greater than 3.6 nm, the photoelectron yield originating from the Au substrate underneath an 18 nm-thick TPBi overlayer was detected, and the hole injection barrier at the “buried” Au-TPBi interface was also successfully determined from a single PYS spectrum. This result demonstrates that PYS is a potentially promising technique for surveying the electronic structures of general buried interfaces, not only organic-electrode interfaces but also e.g. donor-acceptor organic heterojunctions, inside several tens of nm-thick organic electronic devices.

Acknowledgements

The authors would like to thank Mr. U. Hörmann of the University of Augsburg for his help during the CHA-UPS experiments. Financial support from the Joint Studies Program [23–551] of IMS, the G-COE Program (Advanced School for Organic Electronics; G-3) of Chiba University, JSPS KAKENHI [No. 21245042], and the FIRST Program of Kyushu University are gratefully acknowledged. This work was also partially supported by JSPS KAKENHI [23750209], the TEPCO Memorial Foundation, the Yazaki Memorial Foundation for Science and Technology, a Sasagawa Scientific Research Grant [24–233] from JSS, and Izumi Science and Technology Foundation.

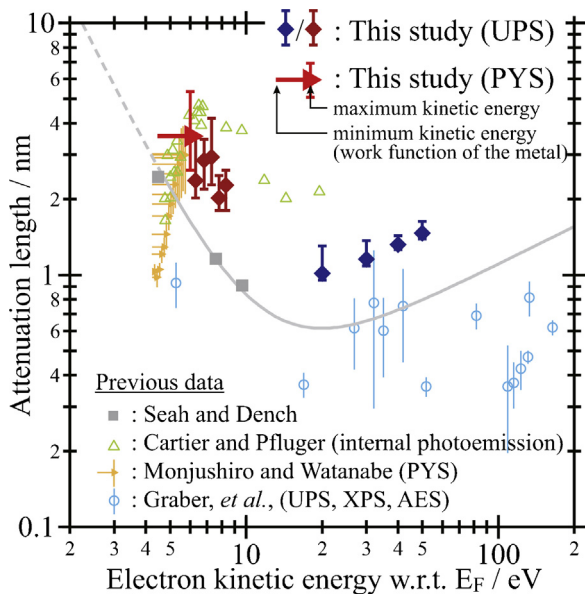


Fig. 5. The AL values obtained in the present study plotted as a function of E_k . The values reported in previous studies for organic materials are also shown, where the density of TPBi is assumed to be 1.26 g/cm^3 to convert the vertical axis of the data set of Seah and Dench [9], the energy difference between the lowest unoccupied energy and Fermi level (4.4 eV) was added to energy standard for Cartier and Pfluger [19], the work function value (4.23 eV) was added to the energy scale for Monjushiro and Watanabe [20], and the one monolayer thickness of PTCDA was assumed to be 0.322 nm to unify the vertical scale [21]. The vertical error bars of the present data sets represent the uncertainties of the AL estimation which was caused by scattering of the data sets, while the left ends of the horizontal bar attached to the PYS results (ours and Ref. [20]) indicates the lowest possible E_k contributing to the PYS signal that is identical to the work function of the respective samples.

References

- [1] H. Sirringhaus, *Adv. Mater.* 21 (2009) 3859.
- [2] Y. Nakayama, S. Machida, Y. Miyazaki, T. Nishi, Y. Noguchi, H. Ishii, *Org. Electron.* 13 (2012) 2850.
- [3] R. Hesper, L.H. Tjeng, G.A. Sawatzky, *Europhys. Lett.* 40 (1997) 177.
- [4] E.V. Tsiper, Z.G. Soos, W. Gao, A. Kahn, *Chem. Phys. Lett.* 360 (2002) 47.
- [5] Y. Nakayama, Y.-H. Huang, C.-H. Wei, T. Kubo, S. Machida, T.-W. Pi, S.-J. Tang, Y. Noguchi, H. Ishii, *J. Appl. Phys.* 108 (2010) 053702.
- [6] R. Schlaf, P.G. Schroeder, M.W. Nelson, B.A. Parkinson, P.A. Lee, K.W. Nebesny, N.R. Armstrong, *J. Appl. Phys.* 86 (1999) 1499.
- [7] N. Hayashi, H. Ishii, Y. Ouchi, K. Seki, *J. Appl. Phys.* 92 (2002) 3784.
- [8] Y. Nakayama, T.L. Nguyen, Y. Ozawa, S. Machida, T. Sato, H. Tokairin, Y. Noguchi, H. Ishii, *Adv. Energy Mater.* 4 (2014), <http://dx.doi.org/10.1002/aenm.201301354>.
- [9] M.P. Seah, W.A. Dench, *Surf. Interface Anal.* 1 (1979) 2.
- [10] R. Eguchi, T. Kiss, S. Tsuda, T. Shimojima, T. Mizokami, T. Yokoya, A. Chainani, S. Shin, I.H. Inoue, T. Togashi, S. Watanabe, C.Q. Zhang, C.T. Chen, M. Arita, K. Shimada, H. Namatame, M. Taniguchi, *Phys. Rev. Lett.* 96 (2006) 076402.
- [11] K. Kanai, M. Honda, H. Ishii, Y. Ouchi, K. Seki, *Org. Electron.* 13 (2012) 309.
- [12] Y. Nakayama, S. Machida, D. Tsunami, Y. Kimura, M. Niwano, Y. Noguchi, H. Ishii, *Appl. Phys. Lett.* 92 (2008) 153306.
- [13] B. Boudaïffa, P. Cloutier, D. Hunting, M.A. Huels, L. Sanche, *Science* 287 (2000) 1658.
- [14] H. Yoshida, *Chem. Phys. Lett.* 539 (2012) 180.
- [15] M.P. Seah, S.J. Spencer, *Surf. Interface Anal.* 43 (2011) 744.
- [16] B. Lesiak, A. Jablonski, A. Kosinski, L. Kóvér, J. Tóth, D. Varga, I. Cserny, B. Aszalos-Kiss, G. Gergely, M. Hasik, A. Drelinkiewicz, E. Wenda, *Surf. Sci.* 507-510 (2002) 507.
- [17] S. Tanuma, C.J. Powell, D.R. Penn, *Surf. Interface Anal.* 21 (1993) 165.
- [18] C.J. Powell, A. Jablonski, *Nucl. Instrum. Methods A* 601 (2009) 1.
- [19] E. Cartier, P. Pfluger, *Phys. Rev. B* 34 (1986) 8822.
- [20] H. Monjushiro, I. Watanabe, *Anal. Sci.* 10 (1995) 797.
- [21] T. Graber, F. Forster, A. Schöll, F. Reinert, *Surf. Sci.* 605 (2011) 878.
- [22] Y. Nakayama, Y. Urugami, M. Yamamoto, S. Machida, H. Kinjo, K. Mase, K.K. Rasika, H. Ishii, *Jpn. J. Appl. Phys.* 53 (2014) 01AD03.
- [23] Z.Y. Liu, S.R. Tseng, Y.C. Chao, C.Y. Chen, H.F. Meng, S.F. Horng, Y.H. Wu, S.H. Chen, *Synth. Met.* 161 (2011) 426.
- [24] Z. Wang, P. Lu, S. Chen, Z. Gao, F. Shen, W. Zhang, Y. Xu, H.S. Kwok, Y. Ma, *J. Mater. Chem.* 21 (2011) 5451.
- [25] E.O. Kane, *Phys. Rev.* 127 (1962) 131.
- [26] M. Kochi, Y. Harada, T. Hirooka, H. Inokuchi, *Bull. Chem. Soc. Jpn.* 43 (1970) 2980.